Epistatic relationships reveal the functional organization of yeast transcription factors

Jiashun Zheng, Joris J. Benschop, Michael Shales, Patrick Kemmeren, Jack Greenblatt, Gerard Cagney, Frank Holstege, Hao Li & Nevan J. Krogan

Supplementary Information

Table of Contents

Supplementary Table 1. List of genes included in the E-MAP.

Class	Genes
Site specific DNA binding transcription factors (STFs)	ACA1 ACE2 ADR1 AFT1 AFT2 ARG80 ARO80 ARR1 ASG1 ASH1 AZF1 BAS1 CAD1 CAT8 CBF1 CHA4 CIN5 CRZ1 CST6 CTH1 CUP2 CUP9 DAL80 DAL82 DAT1 ECM22 FKH1 FKH2 FLO8 FZF1 GAL3 GAL4 GAL80 GAT1 GAT2 GAT3 GAT4 GCR2 GIS1 GLN3 GSM1 GTS1 GZF3 HAA1 HAC1 HAL9 HAP1 HAP2 HAP3 HAP4 HAP5 HCM1 HMS1 HMS2 HOT1 IME1 IXR1 KAR4 LEU3 LYS14 MAC1 MAL13 MAL33 MBF1 MBP1 MET28 MET31 MET32 MGA1 MIG1 MIG2 MIG3 MOT3 MSN1 MSN2 MSN4 MSS11 MTH1 NDT80 NRG1 NRG2 OAF1 OAF3 OPI1 PDR1 PDR3 PDR8 PHD1 PHO2 PHO4 PIP2 POG1 PPR1 PUT3 RDR1 RDS1 RDS2 RFX1 RGM1 RGT1 RIM101 RLM1 RME1 ROX1 RPI1 RPN4 RSF2 SEF1 SFL1 SFP1 SIP4 SKN7 SKO1 SMP1 STB1 STB2 STB4 STB5 STP2 STP3 STP4 SUM1 SUT1 SUT2 SWI4 SWI5 SWI6 TEC1 THI2 TOS8 TYE7 UGA3 UME1 UPC2 URE2 WAR1 WTM1 WTM2 XBP1 YAP1 YAP3 YAP5 YAP6 YAP7 YDR049W YDR520C YHP1 YOX1 YRM1 YRR1 ZAP1
General transcription factors (GTFs)	ABF2 AKR2 ARP8 ASK10 BDF1 BDF2 BRE1 BRE5 BUB1 BUB3 BYE1 CCS1 CHD1 CHL4 CIN1 CIN2 CSE2 CTF18 CTF8 CTI6 CTK1 CYC8 DCC1 DOA1 DOT6 EAF3 EAF5 EAF6 EAF7 ECM23 ECM5 EDS1 ELF1 ELP2 GIM4 GIM5 HHF1 HHT1 HHT2 HIR1 HIR2 HIR3 HMO1 HOS2 HST1 HTZ1 IES1 IES3 IES4 IES5 IKI3 IME4 IRE1 ISW2 ITC1 JHD1 JHD2 KIN28 LEO1 LGE1 LSM1 LSM6 MAD1 MAD3 MCM16 MCM22 MDS3 MED1 MFT1 MGA2 MSI1 NHP6A NHP6B NPR2 NTO1 NUT1 OTU1 PAC10 PFD1 PHO23 PMD1 RCO1 REI1 RIM1 RIS1 RPA14 RPA34 RPA49 RPB2 RPB3 RPB4 RPH1 RPO21 RRP6 RTF1 RXT2 SAC3 SAP30 SAS3 SDC1 SDS3 SEC22 SEM1 SET2 SET3 SET7 SGF11 SGF73 SIF2 SIN3 SNT1 SOD1 SOH1 SPP1 SPS18 SPT2 SPT21 SPT23 SPT3 SPT8 SRD1 SSN2 SSN3 STB6 STD1 SUB1 SWD1 SWR1 TBS1 TEA1 TFB2 TFG1 THP2 TIS11 UBP3 UBP6 UBP8 VID22 VPS71 VPS72 YAF9 YBL054W YBR239C YDR026C YDR266C YER130C YER184C YFL052W YFR057W YGR067C YGR071C YIL151C YJL206C YKL222C YKR096W YLL054C YLR027W YLR278C YML081W YML119W YMR111C YNR063W YPL230W YPR013C YPR015C YPR022C YPR115W YPR196W YPT6 YTA7 ZDS1 ZDS2

Supplementary Table 2. Positive and negative interaction counts, for subsets of the TF EMAP. Data for the previously published early secretory pathway (ESP), chromosome biology and kinase/phosphatase EMAPs were included for comparison. P values for the enrichment of negative interactions among STFs were calculated using different reference sets as indicated in the table. For the kinase/phosphatase EMAP, a P value for the enrichment of positive interactions is indicated by (+).

	STF vs STF (Quadrant I)	*GTF vs GTF (Quadrant III)*	*STF vs GTF (Quadrant II)*	*Kin-Pho*	*ESP*	*Chromosome Biology*
Positives (>=2.5)	23	201	158	64	828	2748
Negatives (<=-2.5)	310	1793	1267	167	3324	12545
P to N ratio	0.074	0.11	0.12	0.38	0.25	0.22
N to P ratio	13.48	8.92	8.02	2.61	4.01	4.56
P value	4.2e-9			1.7e-4(+)		reference
*P value**	6.8e-3		reference			
*P value***	<1e-20			reference		
*P value****	2.3e-11				reference	

Supplementary Table 4. Fisher's exact test for the agreement between the genetic interactions derived from the EMAP and the flow cytometer measurements (P-value=0.0007). The genetic interactions are classified into three categories: positive, neutral and negative with the cutoff defined in the table.

	Positive(EMAP) S-score >=2.5	Neutral(EMAP) -2.5<S-score <2.5	Negative(EMAP) S-score <=-2.5	Total
Positive (FACS) $\varepsilon \geq 0.04$	6	0	1	7
Neutral (FACS) $-0.04 < \varepsilon < 0.04$	7	15	17	39
Negative(FACS) $\varepsilon \leq -0.04$	2	3	14	19
Total	15	18	32	65
Percent of consistent pairs	40%	83%	44%	54%

Supplementary Table 5. Strains used in gene expression experiments (all strains are MATα). Single deletion strains with NATR or NATR –GFP marker were made using standard PCR-base gene knockout with either pFA6a-NATMX4 plasmid or pFA6a-TEF2Pr-eGFP-ADH1-Primer-NATMX4 plasmid.

Wild type	can1Δ::STE2pr-SpHIS5 lyp1Δ::STE3pr-LEU2 LYS2+ his3Δ1 leu2Δ0 MET15+ ura3Δ0
Single deletions	msn2Δ::NAT^R-GFP
	swi4Δ::NAT^R-GFP
	gcr2Δ::NAT^R-GFP
	stb1Δ::NAT^R
	phd1Δ::Kan^R
	skn7Δ::Kan^R
	tye7Δ::Kan^R
Double deletions:	msn2Δ::NAT^R-GFP skn7Δ::Kan^R
	swi4Δ::NAT^R-GFP skn7Δ::Kan^R
	gcr2Δ::NAT^R-GFP tye7Δ::Kan^R
	stb1Δ::NAT^R phd1Δ::Kan^R

Supplementary Table 6. Relative growth rate measured in liquid culture for the single mutants in Supplementary Table 5.

Mutants	Average relative growth rate	Standard deviation of relative growth rate
msn2Δ::NATR-GFP	1.014	0.009
skn7Δ::KanR	1.008	0.012
tye7Δ::KanR	1.018	0.010
gcr2Δ::NATR-GFP	0.743	0.010
stb1Δ::NATR	1.040	0.025
phd1Δ::KanR	1.019	0.030
swi4Δ::NATR-GFP	0.909	0.009

Supplementary Table 7. Genetic interactions of the double deletions in Supplementary Table 5 are confirmed by growth curve measurement in liquid culture.

TF1	TF2	Measured relative growth rate of double mutants	Expected growth rate from single deletions	Genetic Interaction	t	p-value
MSN2	SKN7	0.99	1.02	-0.03	-3.80	9.94E-03
TYE7	GCR2	0.50	0.76	-0.25	-36.38	5.03E-07
STB1	PHD1	1.02	1.06	-0.04	-2.66	3.09E-02
SWI4	SKN7	0.84	0.92	-0.07	-13.68	4.47E-07

Supplementary Table 8. Enrichment of the common targets in the genes changed significantly only in double mutants. PSAMs derived by MatrixReduce(Foat *et al*, 2006) from ChIP-chip(Harbison *et al*, 2004) data were used to calculate the binding affinity of the transcription factors(Foat *et al*, 2008). The targets were then defined with an affinity cutoff as described in the Method. The source of the PSAM represents the condition under which the ChIP-chip experiments were performed.

TF1 (source for PSAM)	TF2 (source for PSAM)	Targets of TF1	Targets of TF2	Common targets	Genes changed only in Double deletions	Common targets changed only in double deletions	Enrichment P-value
TYE7(YPD)	GCR2(YPD)	254	227	17	499	4	0.046
MSN2(H2O2Hi)	SKN7(H2O2Hi)	498	624	99	28	1	0.37
SWI4(YPD)	SKN7(H2O2Hi)	391	624	52	113	4	0.016
STB1(YPD)	PHD1(YPD)	34	95	4	6	0	1

Supplementary Table 10. Components of general transcription factor protein complexes.

Complex	Components included in the E-MAP
INO80-C	ARP8 IES1 IES3 IES4 IES5
BDF1/BDF2	BDF1 BDF2
BRE1/LGE1	BRE1 LGE1
BRE5/UBP3	BRE5 UBP3
BUB1/BUB3	BUB1 BUB3
ChrAssem	MSI1
SOD1/LYS7	CCS1 SOD1
PAF1-C	RTF1 LEO1
CIN1/CIN2	CIN1 CIN2
Mediator	SSN2 SSN3 SOH1 NUT1 CSE2 MED1
CTF8/CTF18/DCC1	CTF18 CTF8 DCC1
CTK-C	CTK1
CYC8/TUP1	CYC8
PREFOLDIN	PFD1 PAC10 GIM4 GIM5
Histones(H3/H4)	HHF1 HHT1 HHT2
HIR-C	HIR1 HIR2 HIR3
SET3-C	SIF2 HOS2 HST1 SET3 SNT1
Elongator	ELP2 IKI3
ISW2/ITC1	ISW2 ITC1
TFIIH	KIN28
LSM-C	LSM1 LSM6
MAD1/MAD3	MAD1 MAD3
MiniChrMainten	MCM16 MCM22 CHL4
TREX	MFT1 THP2

RNAPI	RPA14 RPA34
RNAPII	RPB2 RPB3 RPB4 RPO21
SAC3/THP1	SAC3
COMPASS	SDC1 SPP1 SWD1
SAGA	SGF11 UBP8 SGF73 SPT3 SPT8
TFG1/TFG2	TFG1
SWR-C/HTZ1	HTZ1 SWR1 VPS71 VPS72 YAF9
NuA4_acetyl	YAF9 EAF7 EAF6 EAF5 EAF3
NuA3_acetyl	EAF6 SAS3
RPD3C(S)	EAF3 RCO1 SIN3
RPD3C(L)	SIN3 SAP30 CTI6 SDS3 RXT2 PHO23
VID22/YGR071C	VID22 YGR071C

Supporting Figures

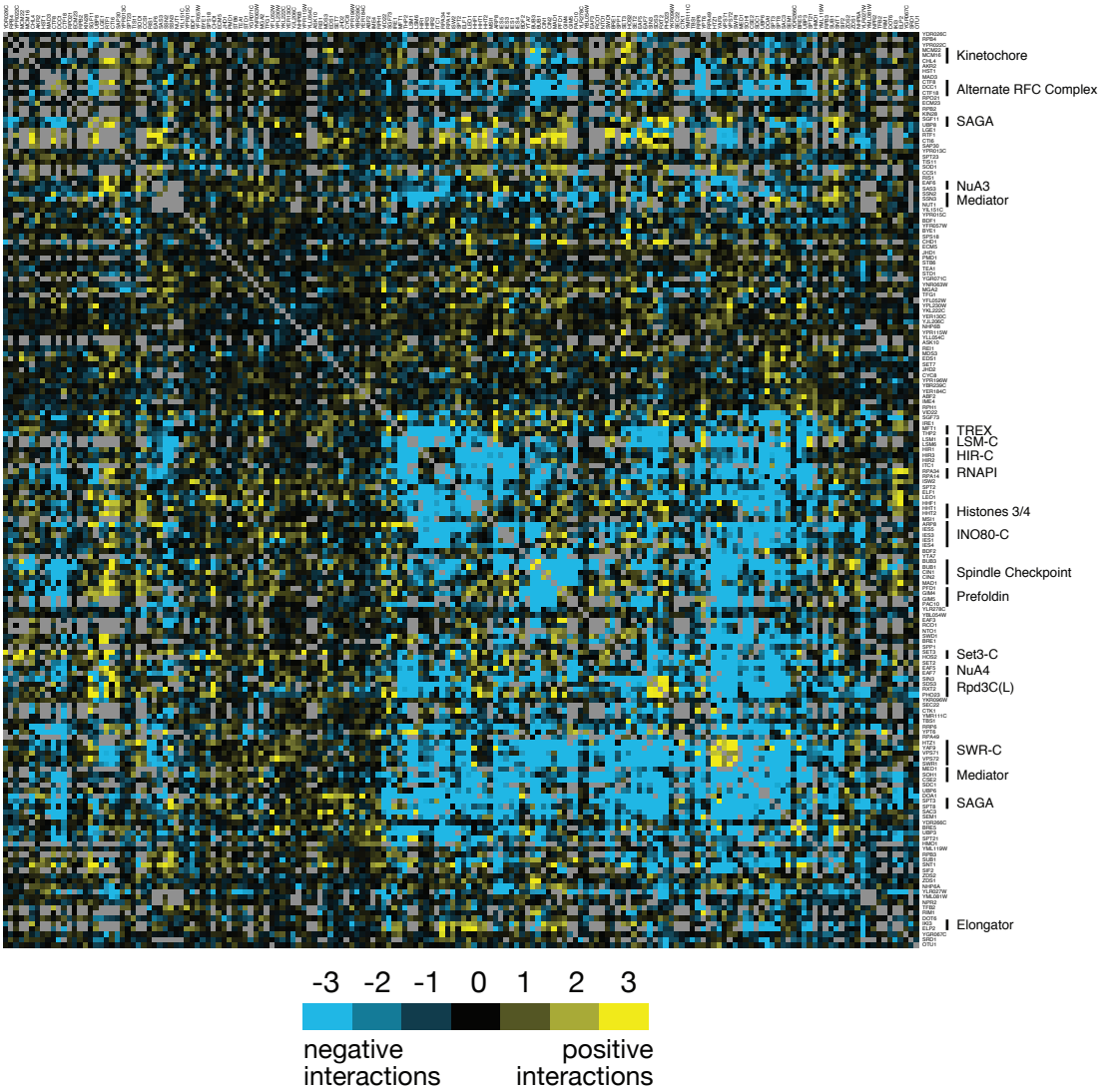

Supplementary Figure. 1. Components of coherently acting complexes cluster together. The general transcription factors are clustered based on their quantitative epistatic interaction profiles. The intensity of yellow and blue indicate the strength of positive and negative interactions, respectively. Several protein complexes are labeled on the genetic clustergram.

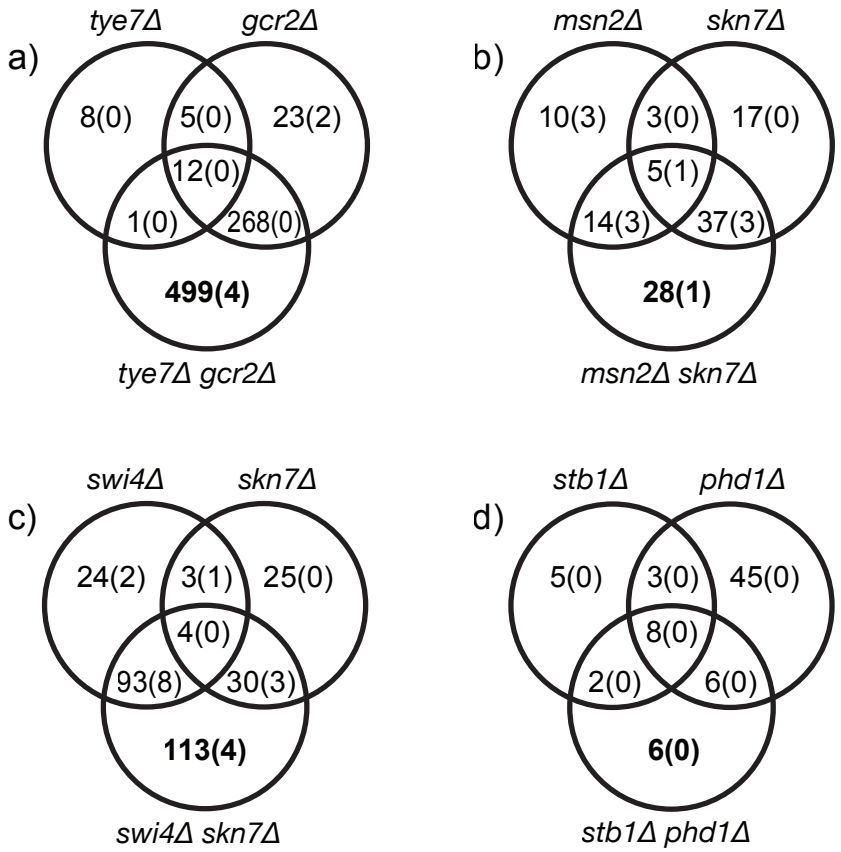

Supplementary Figure. 2. (**a to d**) The number of genes with expression level changed significantly in double mutants and corresponding single mutants. Each sub-figure represents one of the double mutant and its corresponding single mutants in Supplementary Table 5. In each sub-figure, one circle represents the subset of genes changed in the corresponding mutants (compared with wild-type strain). The number of genes changed significantly in the double mutant but not in the corresponding single mutants was shown in the lower circle. Numbers in parenthesis are number of genes predicted to be regulated by both transcription factors. For example, in (**a**). there are 449 genes changed significantly in the double mutant (*tye7Δgcr2Δ*) but not in any corresponding the single mutants (*tye7Δ* or *gcr2Δ* strain), amount them 4 are predicted to be controlled by TYE7 and GCR2.

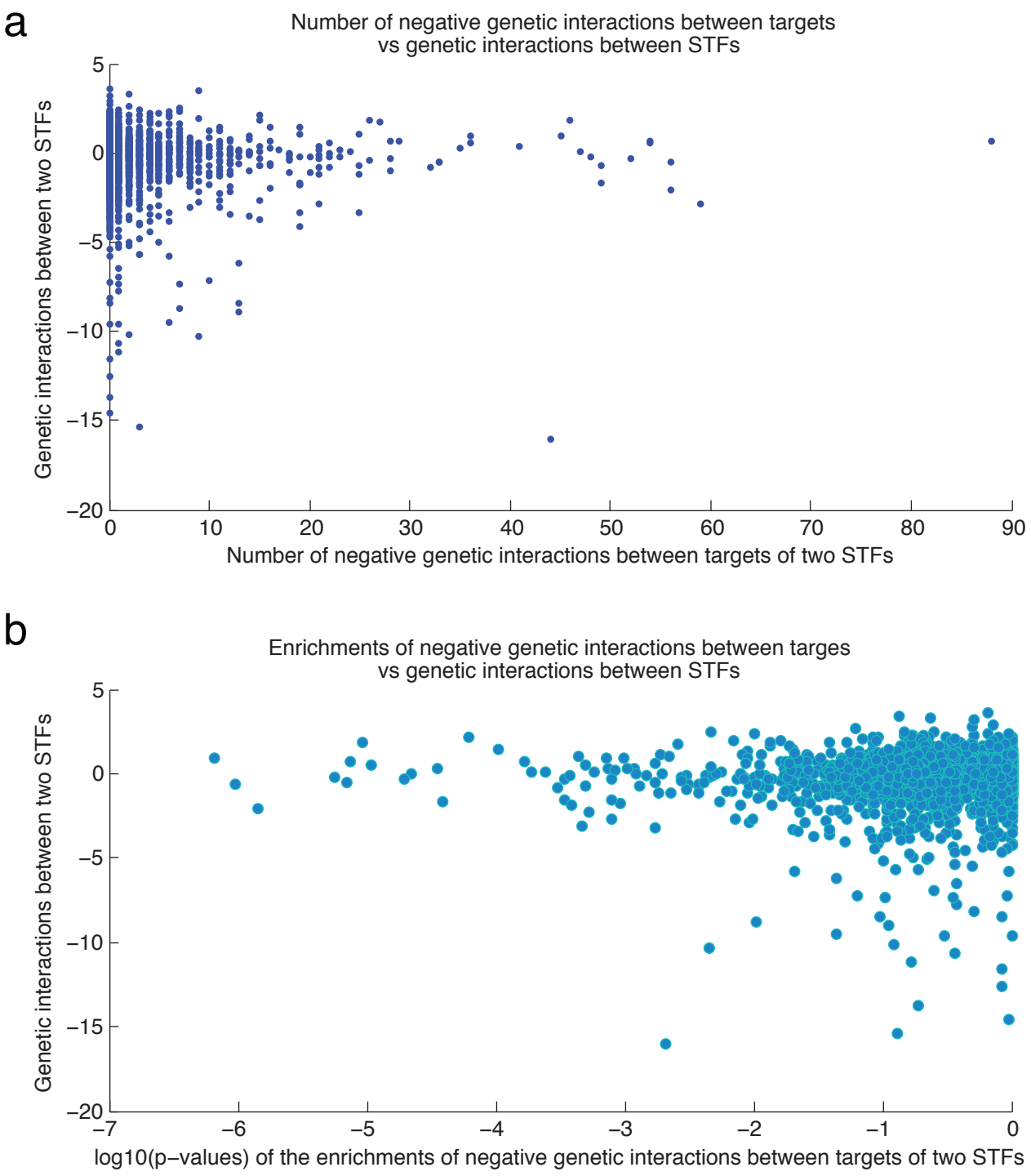

Supplementary Figure. 3 The genetic interactions between two STFs can not be explained by the genetic interactions between their downstream target genes. (a) The genetic interactions between two STFs and the number of negative genetic interactions between their target genes. (b) The genetic interactions between two STFs and the p-values of enrichments of negative genetic interactions between their target genes.

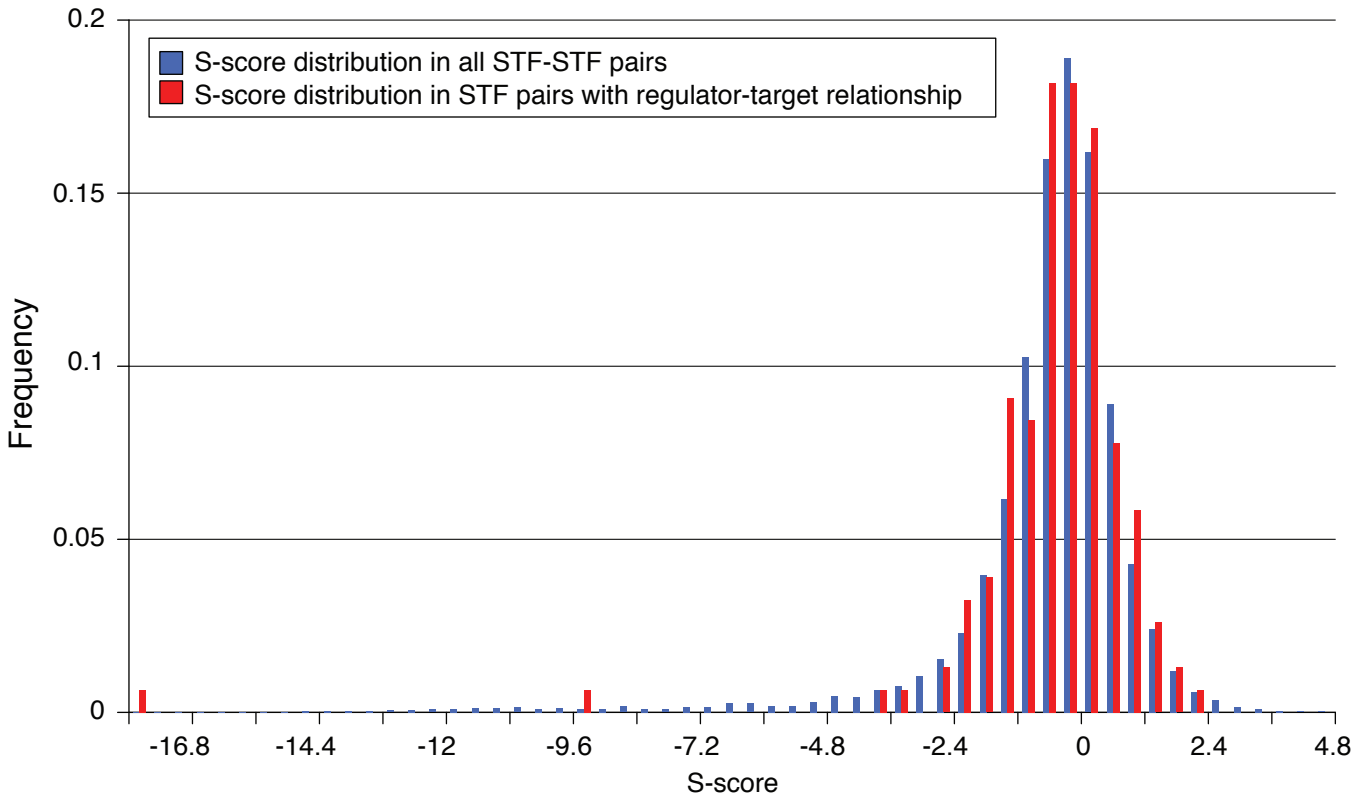

Supplementary Figure. 4. Normalized distributions of the S-scores in all STF-STF pairs (blue) and STF-STF pairs with regulator-target relationship (red). The two distributions are nearly identical.

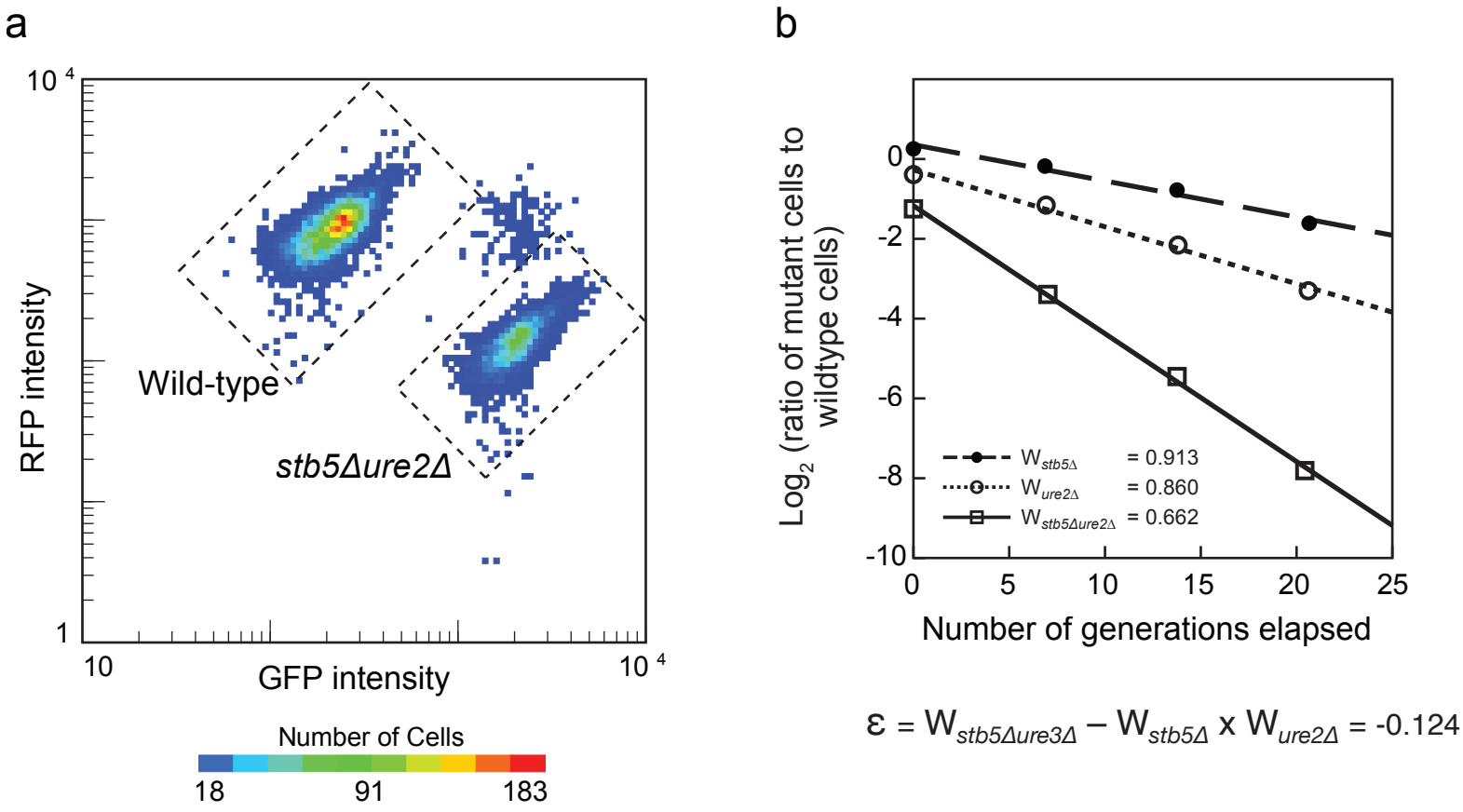

Supplementary Figure. 5. Flow cytometry based measurements of relative growth rates and calculation of genetic interactions. (**a**) An example of scatter plot of GFP vs RFP intensity of cells measured using flow cytometer. RFP-tagged wild-type cells and GFP-tagged mutant cells (*stb5Δure2Δ* in this example) were cultured together in a mixture. The GFP intensity and RFP intensity of the cells were measured by flow cytometer. The two populations of wild-type cells and the mutant cells can be clearly separated by their GFP and RFP intensities (boxed in the plot). The ratio of mutant cells vs wild-type cells was calculated (Breslow *et al*, 2008). (**b**) Measurement of relative growth rate by linear regression of log-ratios vs number of generations. Four time points were measured with the protocol described in Breslow et.al (Breslow *et al*, 2008). The ratio data and derived relative growth rates for the double mutant strain: *stb5Δure2Δ* and its corresponding single mutants (*stb5Δ* and *ure2Δ*) were shown in the figure. The genetic interactions (ε) were then calculated according to the fomular.

Supplementary References

Breslow DK, Cameron DM, Collins SR, Schuldiner M, Stewart-Ornstein J, Newman HW, Braun S, Madhani HD, Krogan NJ, Weissman JS (2008) A comprehensive strategy enabling high-resolution functional analysis of the yeast genome. *Nature Methods* **5:** 711-718.

Foat BC, Morozov AV, Bussemaker HJ (2006) Statistical mechanical modeling of genome-wide transcription factor occupancy data by MatrixREDUCE. *Bioinformatics* **22:** e141-149.

Foat BC, Tepper RG, Bussemaker HJ (2008) TransfactomeDB: a resource for exploring the nucleotide sequence specificity and condition-specific regulatory activity of trans-acting factors. *Nucleic Acids Research* **36:** D125-D131.

Harbison CT, Gordon DB, Lee TI, Rinaldi NJ, Macisaac KD, Danford TW, Hannett NM, Tagne JB, Reynolds DB, Yoo J, Jennings EG, Zeitlinger J, Pokholok DK, Kellis M, Rolfe PA, Takusagawa KT, Lander ES, Gifford DK, Fraenkel E, Young RA (2004) Transcriptional regulatory code of a eukaryotic genome. *Nature* **431:** 99-104.